Silica-Ti3C2Tx MXene Nanoarchitectures with Simultaneous Adsorption and Photothermal Properties

Eduardo Ruiz-Hitzky *, Mabrouka Ounis , Mohamed Kadri Younes , Javier Pérez-Carvajal

Posted Date: 5 June 2024

doi: 10.20944/preprints202406.0225.v1

Keywords: MXenes; Ti3C2Tx; 2D solids; silica; nanoarchitectures; photothermal materials; intercalation; supported reactions

Communication

Silica-$Ti_3C_2T_x$ MXene Nanoarchitectures with Simultaneous Adsorption and Photothermal Properties

Eduardo Ruiz-Hitzky *[1], Mabrouka Ounis [1,2], Mohamed Kadri Younes [2] and Javier Pérez-Carvajal [1]

[1] Materials Science Institute of Madrid (ICMM-CSIC), c/Sor Juana Inés de la Cruz 3, 28049 Madrid, Spain; mabrouka.ounis@etudiant-fst.utm.tn (M.O.); jperez@icmm.csic.es (J.-P.C.)

[2] Laboratory of Materials Chemistry and Catalysis, Department of Chemistry, Faculty of Sciences of Tunis, University of Tunis El Manar, Tunis 2092, Tunisia; younes.mohamedkadri@gmail.com

* Correspondence: eduardo@icmm.csic.es

Abstract: Layered $Ti_3C_2T_x$ MXene has been successfully intercalated and exfoliated with the simultaneous generation of a 3D silica network by treating its cationic surfactant intercalation compound (MXene-CTAB) with an alkoxysilane (TMOS) resulting in a MXene-silica nanoarchitecture that exhibits porosity along with the intrinsic properties of MXene (e.g., photothermal response). The ability of these new materials to produce thermal activation reactions of compounds previously adsorbed on MXene-SiO_2 is shown here. For this purpose, the pinacol rearrangement reaction has been selected as a first model example, testing the effectiveness of NIR laser-assisted photothermal irradiation in these processes. This work shows that Ti_3C_2Tx – based nanoarchitectures open new avenues for applications that rely on the combined properties inherent to their integrated nanocomponents that could be extended to the broader MXene family.

Keywords: MXenes; $Ti_3C_2T_x$; 2D solids; silica; nanoarchitectures; photothermal materials; intercalation; supported reactions

1. Introduction

MXenes are a relatively recent broad family of inorganic solids discovered at Drexel University[1] consisting of two-dimensional (2D) transition-metal carbides, nitrides and carbonitrides of $M_{n+1}X_n$ (n = 1–3) general formula, where "M" represents transition metals (e.g., Ti, Zr, Ta, Nb, V, Mo, Cr, etc.) and "X" are carbon and/or nitrogen elements. MXenes are obtained from the so-called "MAX" phases (layered ternary carbides and nitrides with a general formula $M_{n+1}AX_n$, where "A" represents elements from the group 13 and 14 of the periodic table). The etching of these A-elements generates a large family of MXenes endowed with attractive physicochemical properties combining excellent hydrophilicity and high electrical conductivity as well as intercalation ability, large redox active surface area, rich surface chemistry functionality, and outstanding mechanical properties.[1–6] MXenes are a big family of sustainable and even biocompatible materials that are nowadays considered as promising candidates for the replacement of graphene and other carbon-based 2D materials. MXenes are currently being thoroughly investigated for their uses in a wide range of applications, such as energy storage and conversion, electronics, sensor devices, biomedicine, environment preservation and catalysis.[7,8] Except the electrical conductivity, they exhibit comparable properties to clays and clay minerals, receiving the nickname of "conducting clays" or "carbide clays".[9] However, the term "clay" should preferably be associated to silicates and related small-size particles present in the geosphere.[10]

Based on their intercalation and delamination properties, clay phyllosilicates and MXene carbides/carbonitrides can both be considered today the most representative 2D inorganic solids that are capable to generating a wide variety of nanoarchitectured materials. This feature facilitates interactions between the single layers of these solids with various inorganic species (e.g., metal and

 doi:10.20944/preprints202406.0225.v1

metal-oxide nanoparticles), as well as with many diverse organic compounds, giving rise to organic-inorganic hybrid materials.[10,11]

2. Materials and Methods

Ti_3AlC_2 (MAX phase, 200 mesh powder, from Shanghai Epoch Material Co.). Chemical reagents provided by Sigma-Aldrich and used without further purification: tetramethyl orthosilicate (TMOS) and LiF (analytical reagents grade), NaOH (97% purity, pellets), hydrochloric acid (37.5% wt. HCl), cetyltrimethylammonium bromide (CTAB) (≥98%), tetramethylammonium hydroxide (TMAOH) (25 wt. % in H_2O). Sulfuric acid (95-97%, Merck), pinacol (98%, Aldrich), 2,4 dinitrophenylhidrazine (*purum* quality) provided by FEROSA.

Synthesis of MXene

In a PTFE vial, 0.80 g of LiF was dissolved in 10 mL of 9 M HCl under continuous stirring, and then 0.25 g of Ti_3AlC_2 (MAX) was gradually added into the mixed solution and reacted at room temperature for 72 h. Then, the acidic product was neutralized using 11 M NaOH until pH ≥ 7, incorporating also 4 mL TMAOH as etchant agent. The product obtained was then repeatedly washed with deionized water and methanol with centrifugation at 3500 rpm. Finally, after more than one hour of continuous centrifugation, the resulting $Ti_3C_2T_x$ MXene was collected from a concentrated dark green supernatant solution.Synthesis of MXene-CTAB and MXene-CTAB-SiO_2

100 mg of $Ti_3C_2T_x$ MXene was dispersed in 10 mL of deionized water and added to 10 mL of 7.08 mM cetyltrimethylammonium bromide (CTAB) solution under stirring for 3 days at room temperature. The suspension was then centrifuged at 3500 rpm and the precipitate was dried at 60 °C overnight to obtain the MXene-CTAB sample. For the MXene- CTAB- SiO_2 preparation, the acquired MXene- CTAB was homogeneously dispersed in isopropyl alcohol. Then, an equimolar amount of the alkoxysilane (1:1 MXene/silane) was slowly added to the suspension under continuously stirring for 10 min. Subsequently, water and methanol were dropwise added to the system with a molar ratio of TMOS/H_2O/methanol of 1:2:2. This mixture was kept under magnetic stirring for 72 h at room temperature, then centrifuged and dried.

Removal of CTAB surfactant

The extraction of CTAB from MXene-CTAB-SiO_2 was performed in ethanol solution containing 0.1 M HCl at 70°C for 24h. The dried sample has been named MXene-SiO_2.

Characterization techniques

Powder X-Ray diffractograms was collected in a Davinci instrument form BRUKER in the range between 4 and 70^0 (2θ) angles. FE-SEM images were recorded in a FEI NOVA NANOSEM 230 equipped with an EDAX-Ametek detector. TEM images and EDX were obtained with a JEOL JEM-1400 Plus electron microscope. Nitrogen adsorption isotherms at 77K was recorded in a Micromeritics 3Flex instrument after outgassing the solid powder at 120 º C during 12 hours under vaccum. Attenuated total reflection Fourier transform infrared spectroscopy (ATR-FTIR) was performed using an ALPHA II spectrometer (Bruker Corporation, Massachusetts, USA). The spectra were acquired between 500 and 4000 cm^{-1} with a sample scan time of 256 scans and a resolution of 4 cm^{-1}. Five replicates were acquired for each sample.

Photothermal properties

To investigate the photothermal properties of the prepared MXene and MXene derivatives, they were irradiated with 808 nm wavelength laser light (830 mW). The temperature was continuously recorded for 2 min, then the light source was switched off until the temperature decreased to room temperature. Throughout the irradiation process, thermal images and temperatures changes in the materials were captured with an infrared thermal camera (HIKMICRO).

 doi:10.20944/preprints202406.0225.v1

The photothermal activation of pinacol transposition reaction to pinacolone was carried out dropping saturated pinacol solution on onto H_2SO_4-doped MXene-SiO_2, the sample was exposed to an attenuated NIR laser to heat a pressed millimetric disc of powder ca. 80 °C during 10 minutes. Thin discs of the powdered product were shaped by applying 4 tons/cm^2 for 10-20 seconds in a mechanical press. The detection of the formation of carbonyl compounds from pinacol was performed qualitatively by dropping 2,4-dinitrophenylhydrazine (2,4-DNP) into the isopropanol extracted phase. The formation of a yellow-orange precipitate confirms the presence of a carbonyl group (C=O) in the pinacolone molecule.

3. Results

The controlled arrangement of nano-sized structural units based on nanoarchitectonic approaches is receiving a major boost in the design of advanced functional architectures.[12] In this sense, 2D solids with intercalation and delamination properties that could involve surface interactions of their single layers, present extraordinary potential as building blocks for these purposes.[13] In this way, layered silicates (clay minerals) and more recently MXenes are excellent candidates for generating different functional nanoarchitectures.[10,14] The exfoliation/delamination of 2D solids allows further conformations as films (restacking) or foams (freeze-drying), which in addition to their ability to assemble diverse nanoparticles, polymers or biological fragments, can generate functional nanoarchitectures suitable for a wide range of applications, from reinforcement of polymeric matrices and membrane technologies to several transport properties, like optical, electronic, magnetic, etc.[15–17]

The possibility of designing complex systems with individual layers of different 2D solids highly dispersed in silica matrices allowing to combine their textural properties (high specific surface area and porosity) with the inherent properties of the 2D solid, represents a very attractive opportunity. For example, delaminated clay minerals and related solids, like layered double hydroxides, associated with silica generated by sol-gel processes have been a breakthrough in the production of clay-silica nanocomposites with synergistic properties of both components, i.e., surface properties of the silica and ion exchange properties of the involved clay mineral.[18–21] Intermediate phases of 2D solids modified by the intercalation of cationic alkylammonium species (e.g., hexadecyltrimethylammonium bromide, CTAB) have been found to generate an organic-inorganic interface that facilitates the association and stabilization of alkoxysilanes, and other alkoxides, providing a suitable environment for the subsequent hydrolysis and controlled polycondensation of the alkoxides to form 3D silica networks.[21–22] In addition to alkoxysilanes, Al- and Ti-based alkoxides, as well as other types of metalorganic precursors, have also been successfully used to introduce selected functionalities (acidity, photoactivity, etc.).[23–28] Previous systems dealing with the assembly of MXenes and silica have been successfully produced by co-intercalation of tetraethyl orthosilicate (TEOS) with long chain alkylamines. The resulting materials have been consolidated by calcination giving rise to $Ti_3C_2T_x$ MXenes with SiO_2 pillars being characterized by a permanent increase of the basal interlayer spacing up to 3 nm, as indicated by the corresponding XRD patterns. These materials also show a significant increase in their specific surface area, reaching values greater than 200 m2 g−1. [29,30]

Herein, we report the synthesis of new nanoarchitectures derived from Ti_3AlC_2 carbide (MAX phase) leading to a high dispersion of $Ti_3C_2T_x$ MXene single layers within a silica framework generated from tetramethyl orthosilicate (TMOS). This procedure involves the preparation of an intermediate phase by intercalation of the MXene by the cationic surfactant CTAB (MXene-CTAB) that facilitates the exfoliation and subsequent assembly with the SiO_2 generated by the hydrolysis and condensation of TMOS (Figure 1). The resulting MXene-silica nanoarchitectures are materials that simultaneously exhibit high porosity and photothermal properties inherent to the MXene layers.

 doi:10.20944/preprints202406.0225.v1

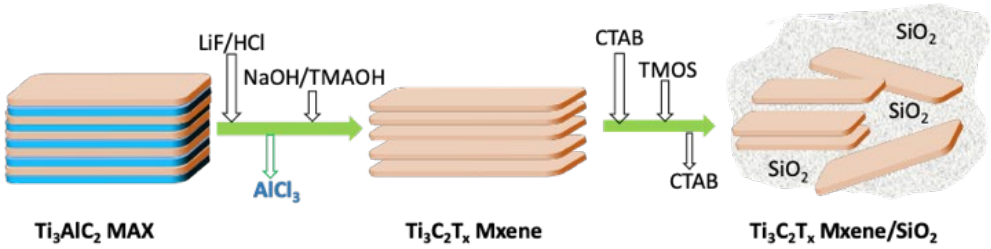

Figure 1. Scheme of the pathway adopted for the synthesis of MXene-SiO_2 nanoarchitectured materials starting from Ti_3AlC_2 carbide (MAX phase) in several steps involving the use of the MXene-CTAB intermediate and the TMOS hydrolysis reaction..

The general procedure followed to prepare the MXene-silica nanoarchitectured materials (Figure 1) is inspired on our previously developed protocol on the preparation of clay-silica nanocomposites.[18,30] The initial first step of the overall process consists in the transformation of the MAX phase (Ti_3AlC_2) into the $Ti_3C_2T_x$ MXene by treatment with LiF dissolved in concentrated HCl to produce the etching of the Al layer of MAX, according the procedure first reported by Ghidiu and co-workers[11], followed by the neutralization of the resulting products with dilute NaOH. At this stage, it is also used here tetramethylammonium hydroxide (TMAOH) as both, neutralizing and etchant agent, taking into account the amphoteric nature of Al^{3+}, which can be extracted from the MAX structure leading to MXenes with $Al(OH)_4^-$ species as terminal groups.[31] In a second step, the cationic surfactant (CTAB), is intercalated in the fresh resulting MXene with the aim to expand its interlayer spacing and facilitate the further access of the TMOS alkoxide used as a silica source. Once MXene-CTAB-SiO_2 nanocomposite are generated, the extraction of the surfactant by treatment with a mixture of ethanol/HCl solutions give rise to MXene-SiO_2 nanoarchitectures. Details of these reactions carried out in the laboratory under mild conditions. The powder X-Ray diffraction (PXRD) patterns (Figure 2a) confirm the formation of the $Ti_3C_2T_x$ MXene from the MAX phase by reaction with LiF/HCl solution[9]. The characteristic diffraction peak assigned to (002) plane is broader and shifted to lower angles in comparison to the one present at the MAX phase indicating an increase in the interlayer distance (d_L) from 0.91 to 1.45 nm. This fact points to the removal of the Al layer from Ti_3AlC_2, subsequently confirmed by EDX analyses (*vide infra*). In addition to plane (002), planes (103) and (105) belonging to the layered carbide structure are clearly identified in the resulting material and are shown here at 0.23 and 0.20 nm, respectively. A similar profile has been recently reported by Wang and co-workers[32] interpreting such diffractogram as indicative of an incomplete etching of the MAX phase based on the presence of remaining peaks assigned to (103) and (105) planes. However, the energy-dispersive X-ray spectroscopy (EDX) results (Figure S1 and Figure S2, ESI) show a low Al content (≤ 2 wt. %) in the etched MAX sample (Figure S3, ESI), proving the extraction of the majority Al layer. The elemental composition of the prepared MXenes also shows the presence of trace amounts of Cl (2.3 wt. %) and the existence of a large amount of F (9.8 wt. %) and O (25.1 wt. %), suggesting that the terminal surface groups (Tx) are mainly −O and −F terminations. EDX results from TEM. The observed increase on the basal spacing after Al extraction from the MAX phase can be attributed to intercalation between the MXene sheets of water molecules and cations, i.e. Li^+ from LiF, Na^+ and TMA^+ from the corresponding hydroxides used for controlling the pH dispersion,[9,33] in addition to methanol molecules further used in the process that could co-intercalate with H_2O molecules playing an active role in the subsequent delamination/exfoliation and facilitating the access of reagents to the interlayer region.

After treatment with CTAB and TMOS driving to the MXene-CTAB-SiO_2 intermediate nanocomposite, the diffraction peak assigned to the (002) plane widens further, while a broad hump appears centred at approximately 22º (2θ degrees), which is characteristic of the amorphous silica produced by the hydrolysis of the alkoxides (TMOS), in accordance with the Standards Joint Committee on Powder Diffraction (JCPDS) corresponding to the standard pattern of amorphous SiO_2.[34] The presence of CTAB is evidenced from the ATR spectra, showing the characteristic peaks at 2922, 2850, and 1460 cm^{-1} that are respectively assigned to the asymmetric and symmetric

 doi:10.20944/preprints202406.0225.v1

stretching vibrations of C–H (ν_{asym}(-CH_2) and νs(-CH_2)) and δ (-CH_2) bending vibrations of methylene groups in the CTA^+ species assembled to the MXene. The intense IR bands at around 1060 cm^{-1} are attributed to the ν_{Si-O} stretching vibrations of silica siloxane bonds. (Figure S4, ESI)

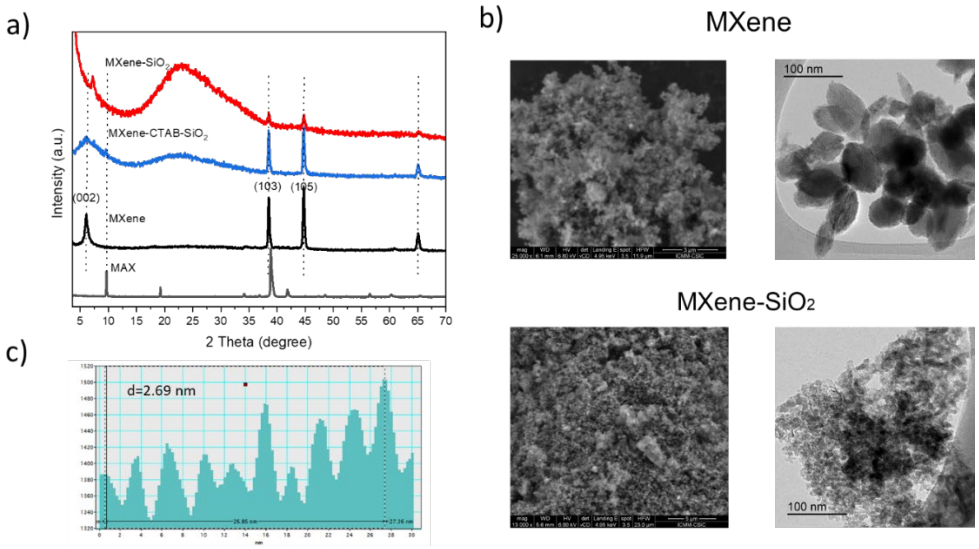

Figure 2. a) XRD patterns of: $Ti_3C_2T_x$ MAX phase, Ti3C2Tx MXene resulting from the MAX phase by reaction with LiF/HCl solution, MXene-CTAB-SiO_2 intermediate compound, and MXene-SiO_2 nanoarchitecture after removal of CTA^+ species; b) FE-SEM (left columns) and TEM images (right columns) of MXene and MXene-SiO_2, respectively; c) Line Profile corresponding to the MXene sample resulting from graphical treatments of the TEM image.

The MXene-SiO_2 nanoarchitecture is finally produced after the removal of CTAB, included as CTA^+ cations in the MXene-CTAB-SiO_2 sample, which is achieved by treatments with ethanol/HCl mixture. The XRD pattern (Figure 2a) shows a broad band centred at 22° (2θ) attributed to amorphous silica along with a broad peak at 6.08° (2θ) corresponding to the (002) plane of the layered carbide. The latter signal appears here with a relatively small intensity compared to the intensity of the other observed reflexions of the carbide (i.e., the (103) and (105) planes). The broadness of the peak corresponding to the (002) plane can be attributed to the distinct interlayer distances produced by the silica access to the MXene interlamellar spacings. The resulting spacings vary over a wide range, the MXene layers being poorly ordered that result in structural disorganization in the stacking of the carbide single layers. Figure 2b shows a representative TEM image of MXene-SiO_2 samples including the corresponding Line Profile (Figure 2c) that could be related with the d-spacings of 2D solids[35], which indicates here an estimated average distance between consecutive planes of d=2.7 nm, the observed increase of this interlayer distance being attributed to the incorporation of silica in the interlayer region. This value measured from the Line Profile deduced from TEM images, should be taken with caution since it is not the result of measurements by conventional diffraction techniques, but it represents an approximation that is consistent with results obtained from related MXene-silica systems.[29] It should also be considered that a partial MXene exfoliation or delamination is also produced, whose identification by TEM in the silica matrix would be very difficult to observe due to the very thin single layer thickness of the carbide together its folding ability leading to corrugated/rolled solids. The effectiveness of the CTAB extraction is confirmed by ATR spectroscopy as it shows the absence of C-H vibrations typical of the cationic surfactant (Figure S4, ESI, which was detected in the intermediate MXene-CTAB sample).

FE-SEM/EDX results of the MXene-derived nanoarchitectures show the dispersion of the layered carbide among the silica particles. At higher magnifications, it is observed that the latter nanoparticles are closely associated with the MXene and, in good agreement with the XRD results, the 2D carbide should be present as a MXene few-layers or as a disordered/delaminated solid dispersed on the generated silica matrix. Figures 2b shows FE-SEM and TEM images of the synthetized MXene and the MXene-SiO_2 nanoarchitecture. In the latter sample, TEM images show a certain organisation in

 doi:10.20944/preprints202406.0225.v1

the stacking of the MXene layers, which appears as a nanostructured solid with an almost regular 00l arrangement that periodically repeats at layer spacings of about 2.7 nm (Line Profile, *vide infra*) (Figure 2c). This expansion is attributed to the interlamellar insertion of silica *in situ* generated by the hydrolysis of TMOS in an environment of the MXene layers with CTA^+ cations as intercalated species. Semi-quantitative EDX analytical results point out to a relatively high content of the Ti and Si elements (belonging to carbide and silica, respectively) as well as a low content of Al compared to the starting MAX phase. An appreciable amount of O and F content is also detected, the former being associated to the assembled silica and the latter consisting mainly of -F terminations. Elements such as Al, Ca, etc., which could contribute to insolubilize fluorides, are not detected, supporting the assignation of –F as T_x terminations in the MXene layers (Figure S2, ESI).

The resulting MXene-SiO_2 nanoarchitectures show a significant increase in porosity and specific surface area with respect to the pristine MXene showing development of new pores in the range of mesopores (Figure 3). The adsorption of N_2 at liquid nitrogen temperature on MXene-SiO_2 nanoarchitectures shows an type-IV, H1-type isotherms associated with porous materials consisting of well-defined cylindrical-like pore channels or agglomerates of compacts quasi-uniform spheres,[36] meanwhile the pristine MXene can be ascribed as type-III, H3-type ascribed to plate-like aggregates of layers with slit-shape holes in good agreement with the nitrogen adsorption isotherm.

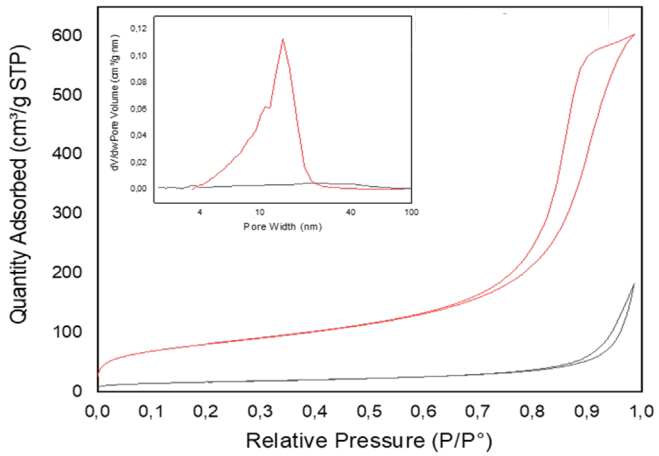

Figure 3. Nitrogen adsorption isotherm and pore size distribution at 77 K of MXene (black) and MXene-SiO_2 (red).

Brunauer-Emmett-Teller (BET) specific surface area measurements show a large increase in surface area from about 60 $m^2.g^{-1}$ in the untreated MXene to above 290 $m^2.g^{-1}$ in the nanoarchitecture (Table S1, ESI) and an average pore width of 12 nm. In relation to this overall increase in the apparent surface area of the material, the pore volume also underwent a considerable increase, i.e. more than 3 times with respect to the initial MXene.

In addition to the development of adsorption capacity, the nanoarchitectures built here should show an effective light-to-heat conversion capacity, more usually known as photothermal conversion, assured by the presence of MXene. This property is a topic that is attracting increased interest focusing important applications such as steam generation, water desalination and cancer therapy.[7,37] Photothermal conversion is also remarkable in nanocomposite materials such as those containing biopolymers (e.g., nanocellulose) assembled to MXenes, which incorporate thermoelectric properties useful in biomedicine and even in amazing behaviors such as controllable light-driven photothermal properties inherent to their 2D carbide component.

 doi:10.20944/preprints202406.0225.v1

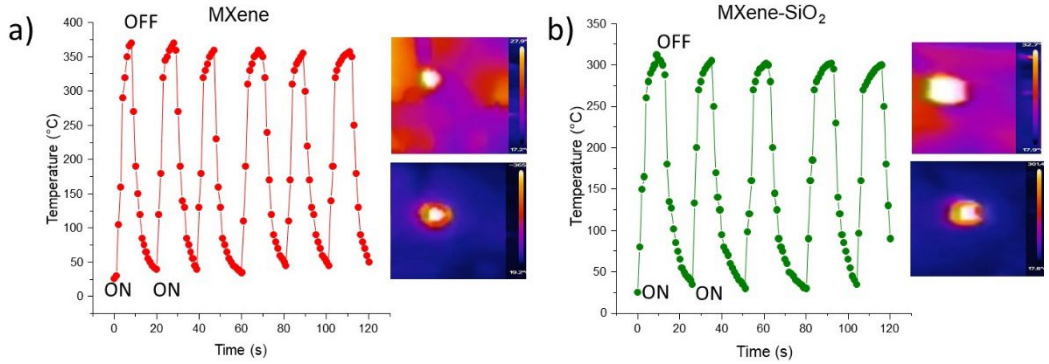

Figure 4. Photothermal cycles upon near infrared irradiation on MXene (a) and MXene-SiO_2 (b) and maximum and minimum temperature pictures.

Cyclic on-off laser irradiation at regular time intervals shows the concomitant increase in temperature (Figure 4) demonstrating excellent repetitive photothermal response activity over long periods of time. We have found that this activity is maintained by storing the samples at atmosphere without special storage precautions at least one year after preparation.

The multifunctionality of the MXene-SiO_2 materials, i.e. their high porosity, together with the properties conferred by the inclusion of the MXene, are of interest in terms of their potential photoactivity and electrical conductivity. These properties are theoretically promising for potential applications such as e.g. active phase of sensors, porous electrodes, heterogeneous catalysis, etc.[38]

Interestingly, the MXene-SiO_2 nanoarchitectures prepared here retain the characteristic photothermal properties of the MXene component together the surface properties of the associated porous silica. In this regard, we have shown that the adsorption of organic molecules on MXene-SiO_2 can be further transformed following a photothermal activation based on NIR laser irradiation. Thus, in a preliminary approach consisting in the adsorption of 2,3-dimethylbutane-2,3-diol, (pinacol) on MXene-SiO_2, after acid doping and NIR laser irradiation a fast and efficient rearrangement reaction to 3,3-dimethylbutan-2-one (pinacolone) was observed in a similar way as it takes place in liquid phase or adsorbed on porous solids.[39], [40,41] As it is well known, the rearrangement reactions of 1,2-diols catalyzed by mineral acids or Lewis solids represent a classical model in organic chemistry,[39] where thermal activation has been traditionally achieved by heating in a conventional oven or under microwave irradiation.[42] In the present case, a very short time (10 minute) irradiation with a NIR laser attenuated to heat at 80-100 ºC on H_2SO_4-doped MXene-SiO_2 containing adsorbed pinacol, produces its rapid transformation in pinacolone, as detected by the 2,4-dinitrophenylhydrazine test with formation of orange colored 2,4-dinitrophenylhydrazone.[39]

4. Conclusions

A new approach for the development of photothermally responsive porous nanoarchitectures by assembling exfoliated $Ti_3C_2T_x$ MXene by intercalation of CTAB with silica generated by hydrolysis of an alkoxysilane (e.g., TMOS) is presented here. It is clearly necessary to extend this initial work, which at this stage could be considered as a proof-of-concept. In this way, future developments could be envisaged by incorporating different types of MXenes and various porous systems capable of assembling at the nanoscale to preserve their inherent photoactive response characteristics and simultaneous surface adsorption properties.

Moreover, the presence of porous silica offers the possibility of further functionalization, for instance by anchoring functional groups via silanization or by the inclusion of enzymatic systems within the large pores generated in these nanoarchitectures. These possibilities open up much broader perspectives for the design and preparation of new multifunctional materials for many different applications, as for instance, active phase of sensor devices. On the other hand, although the current MXene-SiO_2 nanoarchitectures have a very low electrical conductivity (practically undetectable, due to the elevated content in insulating silica), it can be considered to be increased it

 doi:10.20944/preprints202406.0225.v1

future works by incorporating to these nanoarchitectures highly conductive carbon nanoparticles (e.g. MWCNT and GNP), with the aim to drastically improve these properties, as already achieved in related systems.[43]

Further research is needed to ratify and extend the preparation processes of this type of innovative materials based on MXene-derived nanoarchitectured porous systems as initially described here, where a simple model reaction of thermal activation has been selected. This represents only a first example that opens broad application possibilities to different catalytic and non-catalytic organic reactions amenable to photothermal activation.

Supplementary Materials: The following supporting information can be downloaded at: www.mdpi.com/xxx/s1. Figure S1: Energy-dispersive X-ray spectroscopy (EDX) of MXene; Figure S2. Energy-dispersive X-ray spectroscopy; Figure S3. FE-SEM image of Ti3AlC2 (MAX) (EDX) of MXene- SiO_2; Figure S4. ATR spectra of MXene- SiO2 and MXene- CTAB samples. Table S1**:** Textural characteristics of MXene and MXene- SiO_2 samples.

Author Contributions: E.R.-H.: idea conceptualization, methodology, data interpretation, writing original draft, writing-– review & editing final draft, supervision, project administration, funding acquisition. M.O.: data acquisition, investigation, methodology, formal analysis, review & editing, K. Y.: Formal analysis, investigation, supervision, review & editing. J. P.-C.: investigation, methodology, data curation, formal analysis, writing–original draft, review & editing final draft.

Funding: This research was supported by the MCIN/ AEI/10.13039/501100011033/ and FEDER *una manera de hacer Europa* (MAT2015-71117-R), Spanish project PID2019-105479RB-I00 funded by MCIN/AEI/10.13039/501100011033 and JPC acknowledge financial support from RYC2022-037460-I Ramon y Cajal contract and TED2021-131223B-I00 project funded by MCIN/AEI/10.13039/501100011033 and by the "European Union NextGeneration EU/PRTR". The authors gratefully acknowledge the financial support furnished by the Tunisian Ministry of Higher Education and Scientific Research.

Acknowledgments: The authors acknowledge Dr. Cristina Almansa and Dr. Verónica López of the Research Technical Services at the University of Alicante, Spain, for the TEM images, EDX and Line Profile acquisition of the studied samples. We also thank Ismael Ballesteros of the Microscopy Service at the ICMM-CSIC, Spain, for the FE-SEM images.

Conflicts of Interest: The authors declare no conflicts of interest.

References

1. M. Naguib, M. Kurtoglu, V. Presser, J. Lu, J. Niu, M. Heon, L. Hultman, Y. Gogotsi and M. W. Barsoum, *Adv. Mater.*, 2011, 23, 4248–4253.
2. M. Naguib and Y. Gogotsi, *Acc. Chem. Res.*, 2015, 48, 128–35.
3. B. Anasori and Y. Gogotsi, *2D Metal Carbides and Nitrides (MXenes): Structure, Properties and Applications*, Springer International Publishing, Cham, 2019.
4. M. Naguib, V. N. Mochalin, M. W. Barsoum and Y. Gogotsi, *Adv. Mater.*, 2014, 26, 992–1005; B. Anasori, M. R. Lukatskaya and Y. Gogotsi, *Nat. Rev. Mater.*, 2017, 2, 16098.
5. S. Li, B. Gu, X. Li, S. Tang, L. Zheng, E. Ruiz-Hitzky, Z. Sun,C. Xu, X. Wang, *Adv. Healthcare. Mater.*, 2022, 11-12, 2102367.
6. S. Tang, Z. Wu, X. Li, F. Xie, D. Ye, E. Ruiz-Hitzky, L. Wei, X. Wang, *Carbohydr. Polym.*, 2023, 299, 120204.
7. H. Lu, J. Wang, H. Li, W. Zhou, Q. Yuan and S. Liu, *Mater. Chem. Front.*, 2023, 7, 4372–4399.
8. S. Tang, Z. Wu, G. Feng, L. Wei, J. Weng, E. Ruiz-Hitzky and X. Wang, *Chem. Eng. J.*, 2023, 454, 140457.
9. M. Ghidiu, M. R. Lukatskaya, M. Q. Zhao, Y. Gogotsi and M. W. Barsoum, *Nature*, 2014, 516, 78–81.
10. E. Ruiz-Hitzky and C. Ruiz-Garcia, *Nanoscale*, 2023, 15, 18959–18979.
11. E. Ruiz-Hitzky, C. Ruiz-Garcia and X. Wang, *Chem. Mater.*, 2023, 35, 10295-10315.
12. K. Ariga, *Beilstein J. Nanotechnol.*, 2023, 14, 434–453; E. Ruiz-Hitzky, P. Aranda and C. Belver, in *Manipulation of Nanoscale Materials*, ed. K. Ariga, The Royal Society of Chemistry, 2012.
13. K. Ariga, Q. Ji, J.P. Hill, Y. Bando and M. Aono, *NPG Asia Mater.*, 2012, 4, e17, DOI: 10.1038/am.2012.30.
14. E. Ruiz-Hitzky, P. Aranda and C. Belver, *in Manipulation of Nanoscale Materials*, ed. K. Ariga, The Royal Society of Chemistry, 2012.
15. E. Ruiz-Hitzky, P. Aranda, M. Darder and M. Ogawa, *Chem. Soc. Rev.*, 2011, 40(2), 801–828.
16. P. Aranda and E. Ruiz-Hitzky, *Chem. Rec.*, 2018,18, 1125–1137.
17. Y. Lvov, B. Guo and R.F. Fakhrullin, *Functional Polymer Composites with Nanoclays*, Book Series: RSC Smart Materials. Vol. 22, Royal Society of Chemistry, Cambridge, 2017.
18. S. Letaïef and E. Ruiz-Hitzky, *Chem. Commun.*, 2003, 2996–2997.

 doi:10.20944/preprints202406.0225.v1

19. S. Letaïef, M.A. Martín-Luengo, P. Aranda and E. Ruiz-Hitky, *Adv. Funct. Mater.*, 2006, 16, 401–409.
20. P. Zapata, C. Belver, R. Quijada, P. Aranda and E. Ruiz-Hitzky, *Appl. Catal. A*, 2013, 453, 142–150.
21. M. Djellali, P. Aranda and E. Ruiz-Hitzky, *Appl. Clay Sci.*, 2019, 171, 65-73.
22. P. Aranda and E. Ruiz-Hitzky, *Chem. Rec.*, 2018, 18, 1125–1137.
23. E. Manova, P. Aranda, M.A. Martín-Luengo, S. Letaïef and E. Ruiz-Hitzky, *Micropor. Mesopor. Mat.*, 2010, 131, 252–260.
24. E. Ruiz-Hitzky and P. Aranda, *J. Sol-Gel Sci. Technol.*, 2014, 70, 307–316.
25. J. Perez-Carvajal, P. Aranda, S. Obregón, G. Colón and E. Ruiz-Hitzky, *Micropor. Mesopor. Mat.*, 2016, 222, 120–127.
26. L. Bouna, B. Rhouta, M. Amjoud, F. Maury, M.-C. Lafont, A. Jada, F. Senocq, L. Daoudi, *Appl. Clay Sci.*, 2011, 52, 301-311
27. B. Rhouta, L. Bouna, F. Maury, F. Senocq, M.C. Lafont, A. Jada, M. Amjoud and L. Daoudi, *Appl. Clay Sci.* 2015, 115, 266–274
28. J. Perez-Carvajal, P. Aranda and E. Ruiz-Hitzky, *J. Solid State Chem.*, 2019, 270, 287-294.
29. P. A. Maughan, V. R. Seymour, R. Bernardo-Gavito, D. J. Kelly, S. Shao, S. Tantisriyanurak, R. Dawson, S. J. Haigh, R. J. Young, N. Tapia-Ruiz and N. Bimbo, Langmuir, 2020, 36, 4370–4382.
30. S. Letaïef, M.A. Martín-Luengo, P. Aranda and E. Ruiz-Hitzky, *Adv. Funct. Mater.*, 2006, 16, 401–409.
31. J. Xuan, Z. Wang, Y. Chen, D. Liang, L. Cheng, X. Yang, Z. Liu, R. Ma, T. Sasaki and F. Geng, *Angew. Chem. Int. Edit*, 2016, 55, 14569-14574.
32. B. Wang, Y. Li, H. Hu, W. Shu, L. Yang and J. Zhang, *PLoS ONE*, 2020, 15(4), e0231981.
33. T. Zhang, L. Pan, H. Tang, F. Du, Y. Guo, T. Qiu, and J. Yang, *J. Alloys Compd.*, 2017, 695, 818e826.
34. A. B. Prasetyo, M. Handayani, E. Sulistiyono, A. N. Syahid, E. Febriana, W. Mayangsari, E. Y. Muslih, F. Nugroho and F. Firdiyono, *J. Phys.: Conf. Ser.*, 2022, 2190, 012013.
35. B.S. An, Y. J. Shin, J.S. Ju, C.W. Yang, Appl. Microsc., 2018, 48, 122-125.
36. M. Thommes, K. Kaneko, A-V. Neimark, J-P. Olivier, F. Rodriguez-Reinoso, J. Rouquerol and K. S. W. Sing, *Pure Appl. Chem.*, 2015, 87, 9.
37. R. Li, L. Zhang, L. Shi, and P. Wang, *ACS Nano*, 2017, 11, 3752−3759.
38. S. Tang, Z. Wu, G. Feng, L. Wei, J. Weng, E. Ruiz-Hitzky, and X. Wang, *J. Chem. Eng.*, 2022, 454, 140457.
39. Pinacol rearrangement, Wikipedia. The free Encyclopedia, https://en.wikipedia.org/wiki/Pinacol_rearrangement, accessed March 30th, 2024; IvyPanda. 2021. "The Pinacol Rearrangement Organic Reaction" May 11, 2021. https://ivypanda.com/essays/the-pinacol-rearrangement-organic-reaction/),
40. E. Gutierrez and E. Ruiz-Hitzky, *Mol. Cryst. Liqu. Cryst. Inc. Nonlin. Opt.*, 1988, 161, 453-458.
41. E. Gutierrez, A.J. Aznar and E. Ruiz-Hitzky, *Heterogeneous catalysis and fine chemicals: proceedings of an international symposium*, Poitiers, March 15-17, 1988, Vol.41, 211-219, ISBN: 0-444-43000-8.
42. E. Gutierrez, A. Loupy, G. Bram and E. Ruiz-Hitzky, *Tetrahedron Lett.*, 1989, 30, 945-948.
43. E. Ruiz-Hitzky, M. M. C. Sobral, A. Gómez-Avilés, C. Nunes, C. Ruiz-Garcia, P. Ferreira and P. Aranda, *Adv. Funct. Mater.*, 2016, 26, 7394-7405.